electronics

Article

Maximizing the Electricity Cost-Savings for Local Distribution System Using a New Peak-Shaving Approach Based on Mixed Integer Linear Programming

Hossam Mosbah *, Eduardo Castillo Guerra and Julian L. Cardenas Barrera

Department of Electrical & Computer Engineering, University of New Brunswick (UNB), Fredericton, NB E3B 5A3, Canada
* Correspondence: hmosbah@unb.ca

Abstract: The objective of this study is to perform peak load shaving at a virtual power plant (VPP) to maximize the electricity cost-saving for local distribution companies (LDCs) while satisfying the necessary operational constraints. It can be achieved by implementing an efficient algorithm to control the conservation voltage reduction technique (CVR) with embedded energy resources (EERs) to optimize electricity costs during peak hours. EERs consist of distributed energy resources (DERs) such as solar and diesel generators and energy storage systems (ESSs) such as utility-scale and residential batteries. An objective function of mixed integer linear programming is formulated as the electricity cost function. Different operational constraints of EERs are formulated to solve the peak shaving optimization problem. The proposed algorithm is tested using data from a real Australian power distribution network. This paper discusses four cases to demonstrate the performance and economic benefits of the control algorithm. Each of these cases illustrates how EERs contribute differently each year, month, and day. Results showed that the proposed algorithm offers significant cost savings and can shave up to three daily peaks.

Keywords: energy storage system; distrusted energy resources; virtual power plant; optimization; peak load shaving; peak load leveling; demand response; solar power

check for updates

Citation: Mosbah, H.; Guerra, E.C.; Barrera, J.L.C. Maximizing the Electricity Cost-Savings for Local Distribution System Using a New Peak-Shaving Approach Based on Mixed Integer Linear Programming. *Electronics* **2022**, *11*, 3610. https://doi.org/10.3390/electronics11213610

Academic Editor: Jahangir Hossain

Received: 21 September 2022
Accepted: 2 November 2022
Published: 4 November 2022

Publisher's Note: MDPI stays neutral with regard to jurisdictional claims in published maps and institutional affiliations.

Copyright: © 2022 by the authors. Licensee MDPI, Basel, Switzerland. This article is an open access article distributed under the terms and conditions of the Creative Commons Attribution (CC BY) license (https://creativecommons.org/licenses/by/4.0/).

1. Introduction

The goal of peak load shaving is to flatten the load curve by reducing the amount of load and shifting it to lower load periods. Peak shaving benefits both customers and utilities. Utility companies can obtain a significant cost saving by reducing consumption when electricity charge rates are relatively high, which results in lower electricity bills for their customers [1]. Chao Lu in [2] proposed both charging and discharging control models of battery energy system storage (BESS). These two models were established with two different optimization objectives. The first objective function is to reduce peak load demand and the second is to minimize the daily load variance. The authors also considered the fluctuation of penalty cost in the objective functions. A rolling load forecasting technique was used to improve the optimization performance. A combination of CVR and EV2G reactive power was investigated in [3] to reduce peak load demand while maintaining the voltage profile within limits. A combination of CVR with EV2G reactive power is assessed in three modes: with no CVR, CVR standalone, and CVR with EV2G reactive power. The technique is verified using a modified IEEE 13 node. Simulated results indicate that the CVR standalone operation reduced peak load demand by 2.60%. However, CVR standalone mode at deeper levels of voltage reduction leads to violations of the minimum node voltage limit and higher system losses. Thus, CVR with EV2G coordinated operation is very helpful to maintain feeder voltage profiles within limits and reduce system losses, even at the deepest levels of voltage reduction. Additionally, the simulation results indicate that a combination of CVR and EV2G mode performs better than CVR standalone operation in terms of peak

power shaving, voltage profile improvement, and loss reduction. An integrated scheme combining conservation voltage reduction (CVR) and intelligent photovoltaic inverter control functions is proposed in [4] to reduce substation demand more effectively than with only CVR. IEEE-123 (medium-size) and IEEE-8500 (large-size) unbalanced three-phase distribution systems are considered for evaluating the proposed scheme in conjunction with a voltage-dependent load model. As a result, a higher demand reduction is achieved during the more profound voltage reduction range, which keeps the distribution network reliable and efficient. Chowdhury in [5] studied the effect of combining PV with battery energy storage in standalone mode. Southeastern and western U.S. peak demand curves were reshaped using PV and battery energy storage. Initially, the PV power is used to charge the battery, and then after the battery is fully charged, it is used to supply the grid. Different photovoltaic array orientations are used to demonstrate substantial savings on the size of the battery storage system necessary to reduce peak loads. The results showed that Western U.S. utilities saved a significant amount of battery capacity compared to southeastern utilities. These are 43% for the south-facing scheme compared to 39% for the two-axis tracking scheme. Furthermore, southeastern utilities have somewhat smaller savings. These are 18% for the two-axis tracking scheme compared to 13% for the south-facing array. The authors in [6] proposed an efficient technique known as a decision tree-based technique to reduce peak load in residential networks. PV arrays, battery storage, and coordinated electric vehicle management were utilized with the technique. Smart meters were implemented to read the residential load in real time, allowing the algorithm to take the necessary action. The proposed algorithm demonstrated 96% reduction in the peak demand with 74% load factor. Bidirectional V2G services are proposed in [7–9] for peak load shaving. These services can be achieved with active power support during peak hours. The EV system operates by charging the EV during off-peak hours and injecting extra EV energy into the power grid during peak hours. V2G can provide reactive power for grid voltage regulation in addition to active power. Furthermore, two different results were obtained. Firstly, the maximum peak shaving value at 10:00 a.m. was approximately 10% of the general power load. Secondly, the maximum peak shaving from 2:00 p.m. to 4:00 p.m. was around 9% of the maximum power load. An integrated battery storage system, a PV system, a heat pump system, a thermal storage system, and an electrical storage system was proposed by Baniasadi et al. [10]. A hybrid system is used in a residential building to optimize the real-time energy storage systems. Particle swarm optimization (PSO) is implemented to mitigate both daily electricity and life cycle costs of the smart building. The Min-Max model predictive controller is then used to minimize electricity costs for end users by managing the energy flows of storage systems. A demand response technique is implemented to optimally control HP operation and battery charge/discharge actions. The controller adjusts the flow of water in the storage tank to meet designated thermal energy requirements by controlling HP operation. Additionally, the battery's power flow is controlled to minimize electricity costs during peak-load hours. The proposed methods reduced annual electricity costs by 80% and life cycle costs by over 42%. The authors of [11] presented a smart grid project that aims at reaching 15% of peak load reduction. The project includes both residential and commercial loads, as well as 230 PV panels equipped with large-scale utility storage which utilizes two technologies to provide smoothing capacity of 0.5 MW and storage capacity of 1 MWh. The GridLAB-D software was primarily used for modeling the proposed system. Vanhoudt et al. [12] used a virtual heat pump equipped with PV panels or a small wind turbine to limit the peak load on a single residential building. A second goal was to reduce the curtailment of renewable energy installations. This was achieved by switching on the heat pump whenever the local renewable energy source produces energy (maximizing self-consumption of renewable energy). This reduced the overall use of gray electricity from the grid. An active heat pump was controlled by a market-based multi-agent system (MAS) and compared to conventional heat-driven control of the heat pump. The comparison showed the MAS actively controlled heat pump is able to lower the peak load from 2% to 5% on the coldest week and 17% for an average week.

The Binary Particle Swarm Optimization algorithm (BPSO) was proposed by Sepulveda et al. [13] to schedule power consumption of a domestic electric water heater. The algorithm used to maximize the level of customer comfort while minimizing peak load demand. Matlab is used to simulate the data collected from 200 households by smart meters to test the performance of the demand response. Authors of [14] proposed a peak shaving mechanism that takes into account the interests of utility companies as well as their customers. The energy model and the price model were both employed to optimally schedule individual water heaters. The energy model allowed for a minimum of electricity consumption for water heaters while maintaining user comfort.

An economic analysis was conducted by Martins et al. [15] to determine the optimal sizing and design for BESS based on monthly and annual billing. An analysis of a case study showed that monthly billing reduces battery aging as the number of cycles increases. Furthermore, the results show that batteries can shorten the payback period when used for large industrial loads in peak shaving applications. Cheng et al. [16] used mixed integer linear programming (MILP) to optimize the scheduling problem for peak-shaving hydropower. The proposed technique is validated using six cascaded hydropower reservoirs along the Lancang River in China. A comparison is made with traditional peak-shaving methods that require determining peak-shaving order. A model is tested from an engineering perspective to determine its efficiency and practicality. A new short-term peak-shaving method was introduced by Liao et al. [17] that took into account load characteristics and water spillage to address modeling, solving, and water spillage treatment issues associated with HSCHPs during the wet season. A fuzzy cluster analysis is used to identify the valley periods of the daily load curve to determine when more water should be released. The best WSRs are determined by solving a mixed-integer linear programming model linearized by special ordered sets of type two. It is demonstrated that the proposed method can achieve a reasonable peak-shaving effect without significantly reducing power generation or introducing an additional water spill. A vehicle-to-buildings/grid (V2B/V2G) system was considered simultaneously by the authors in [18] for peak shaving and frequency regulation using a combined multi-objective optimization strategy that considered battery state of charge (SoC), EV battery degradation, and EV driving scenarios. Study objectives included achieving superior economic benefits within controlled SOCs. The authors in [19] developed a control algorithm for a biomass-based micro combined heat and power (mCHP) plant aimed at reducing electricity consumption. Two scenarios of the mCHP's operation, namely with and without the control strategy, are discussed. EnergyPRO software was used to simulate mCHP operation in this study. When power is overproduced due to low demand, excess power is redirected into heat generation, and vice versa. The authors concluded that the proposed mCHP system covers the household's total power demand during the morning peak and reduces the evening peak by up to 71%. The authors in [20] proposed an optimal energy management algorithm (OEMA) to reduce peak load by scheduling EV charging and discharging with PV system, RES, and ESS. The case study focuses on a university campus with EVs, solar panels, and an energy storage system (ESS), in addition to an educational building that has laboratories and a smart parking lot with 100 charging stations. Simulated results indicated that immediate charging impacted the building's power consumption significantly. In contrast, scheduling EV charging with the help of the PV system and ESS decreased the building's on-peak power consumption while minimizing EV charging costs. The work in [21] considered a model predictive control-based multi-objective optimization was considered for a hybrid energy storage system. This model consists of a PV system, a battery, and a combined 60 heat pump/heat storage device. The goal was to minimize operation costs and reduce power exchanged with the electrical grid while maintaining user comfort. As a result, a reduction of 8 to 88% could be achieved in PV grid feed-in depending on PV capacity. Further benefits can be achieved by MPC of multiple components such as PV/battery/heat pump systems or by controlling air source heat pumps.

Prior studies have not addressed the capability of their techniques to shave more than one peak per day or the economic analysis. Therefore, this paper aims to illustrate the capability of the control algorithm to shave more than one peak per day, followed by an economic analysis of peak load shaving.

Two reasons can be attributed to multiple peaks:

- Weather conditions could contribute to multiple peaks on the same day. Customers heavily use devices such as EWH, HP, BBH, and ETS during cold weather. Thus, multiple peaks were caused by an increase in customers' consumption.
- The second reason is energy storage systems. Since the batteries are discharged during peak times, thousands of homes can use less utility power during peak times. However, if the batteries are charged off-peak at the same time, this could result in multiple peaks.

Contribution and Paper Organization

An effective, fast, and beneficial control algorithm for peak load shaving is presented in this paper. Mixed integer linear programming (MILP) is formulated at a virtual power plant level (VPP) to perform peak load shaving in order to minimize the total electricity cost including energy and demand charge costs for local distribution companies (LDCs). The embedded energy resources are optimized to reduce the load demand during peak hours, resulting in increased electricity cost savings. The EERs consist of distributed energy resources and energy storage systems. Distributed energy resources include solar and diesel generators which provide electricity during peak hours to reduce customers' consumption. Energy storage systems such as utility-scale and residential batteries are discharged to reduce the reliance on utility power during peak periods. Additionally, demand response is applied during peak hours to ask customers to limit the use of their EWH, HP, BBH, and ETS devices. Four different cases are discussed to illustrate the performance and the economic benefit of peak load shaving mechanism for LDCs. The control algorithm proved to be capable of shaving up to three daily peaks and maximizing the cost savings over AUD 600,000 a year. Moreover, the control algorithm offers direct benefits to utilities such as stability, reliability, and generation costs.

The rest of the paper is organized as follows: Section 2 presents an introduction of VPP. Section 3 presents the calculations of the initial power threshold. Section 4 discusses the system model of ESSs and DERs presented in this paper. Section 5 presents the mathematical model of the proposed algorithm. Section 6 presents the results of the algorithm. Finally, the paper presents brief conclusions in Section 7.

2. Virtual Power Plant (VPP)

The demand for electricity in developed countries increases, while the construction of new large power plants is significantly slowing down due to high costs and environmental concerns. Therefore, VPPs are designed to dispatch a group of decentralized energy assets that can be remotely controlled as a group but operate independently. Local assets such as solar and diesel generators are dispatched by VPPs for LDCs. As shown in Figure 1, VPPs receive different types of load forecasts which represent forecasting of customers' consumption in order to determine the highest consumption and the time when these assets should be optimized to reduce peak consumption. Afterward, VPPs share peak information with customers so aggregators can be reduced during the peak period by implementing demand response. The VPP has the responsibility of sharing information with the system operator for assessing the entire system's security. The VPPS will request the start and stop of EERs, generation capacity, and optimization of generation costs. Figure 1 shows the entire process of VPPs.There are no clear definitions of VPPs in literature at the moment. According to [22], VPPs consist of different types of distributed resources which may be dispersed across a medium voltage distribution network. VPPs consist of several technologies with diverse operating patterns and availability that can connect to different points in the distribution system [23]. VPPs are defined in the EU's virtual fuel cell power

plant project [24] as a network of interconnected decentralized residential micro-chips that utilize full-cell technology installed in multifamily homes, businesses, and other public buildings for individual heating, cooling, and electricity production. Fenix in [25] defines VPPs as a flexible representation of a portfolio of distributed energy resources (DER) that is capable of making contracts in the wholesale market and provide services to system operators. VPPs are classified into two types: commercial VPP that combines the capacity of a variety of distributed energy resources and optimizes revenue from contracting DERS and demand portfolios. However, this does not take into consideration any aspects of stable operation. The second type is technical VPPs which consist of portfolio inputs from DERs that have the same geographical location to characterize the local network at the transmission boundary. Both the cost and operational characteristics of the portfolio are represented at the transmission boundary. The details about their characteristics and how they were implemented in the framework of the control algorithm are discussed in [26]. We only consider commercial VPPs in this paper. No information was shared with the system operator at the transmission side.

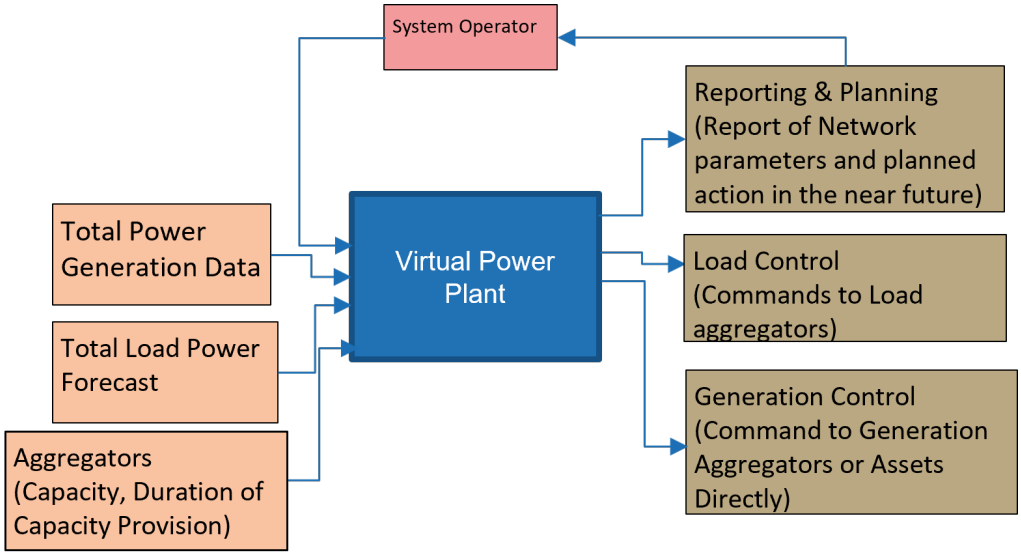


Figure 1. The process of VPPs for LDCs.

3. Load Demand Threshold

The load demand threshold is calculated to determine the peak load hours in the load profile. Time-of-use billing is widely used by utilities to charge their customers. The electricity rate may vary depending on the time of day when it is consumed. On-peak and off-peak times of the day will be defined by the utilities based on the amount of demand at those times. A higher rate is charged to customers during peak hours. Local distribution companies (LDCs) pay for electricity based on both demand charges and consumption charges. A demand charge is determined by multiplying the peak demand rate by the peak demand (kW), and an energy charge is calculated by multiplying the consumption (kWh) by the energy rate. The initial load demand threshold is calculated based on historical data. The calculation is based on previous years in the same month. The initial load demand threshold for February 2021 would be calculated by taking the maximum of the previous years in the same month, for example, the maximum of February 2020 and February 2019, and then taking the average of these two previous months. The final value will be the initial load demand threshold for February 2021. In addition, as the load demand slightly varies from day to day, the load demand threshold is changed. The load demand threshold is updated daily based on the new peak after peak load shaving performance, so if the new peak is at the load demand threshold, the load demand threshold will remain the same for the next 24 h. Otherwise, the peak is partially shaved and the new peak will continue as a new load demand threshold in the next 24 h.

4. System Model

4.1. Aggregators (AGGs)

The energy cost is calculated for each aggregator and then optimized based on its least energy cost during the peak hours. Section 5 described the steps of calculating the energy cost in details. Detailed information on the design and operation of the aggregators can be found in [27].

4.2. Conservation Voltage Reduction (CVR)

The CVR strategy is one of the most efficient ways to reduce load demand and maintain proper voltage. Standalone CVR is used in this paper to reduce the load demand. CVR is selected as the first option to contribute to peak load shaving. Detailed information on the implemented CVR can be found in [4].

4.3. PV Model

Solar irradiation $I_s\ (t)$ data is used to calculate PV output power [28]:

$$P_{PV}\ (t) = I_s\ (t) \times\ A_{PV}\ \times\ N_{PV}\ \times\ \eta_{PV}\ \times\ \eta_t \tag{1}$$

where A_{PV} and N_{PV} indicate the area and the number of PV module, respectively. η_{PV} and η_t represent efficiency of PV system and temperature coefficient:

$$\eta_t = 1 - [\mu(T_c - T_{stc})] \tag{2}$$

where T_c and T_{stc} represent temperature of the PV cell and standard test conditions, respectively. A maximum temperature of T_{stc}= 25 °C indicates the peak of the optimal temperature range for photovoltaic solar panels. This is when solar photovoltaic cells are at their most efficient and expect their performance to be at its best. μ represents temperature coefficient of the maximum output power of the panel 1/degree °C. There is a range of 0.5% to 0.9% depending on the panel; however, 0.005 (0.5%) is an acceptable range. When the temperature of the cell rises above 25 °C, the cell's efficiency begins to decline.

4.4. Diesel Generator

A diesel generator is necessary for the hybrid system to perform as a backup power source. It operates when all embedded energy resources (EERs) are unable to fully shave the load. Diesel generators are the last option because of their high fuel costs:

$$Min \sum_{t=1}^{t_{max}} \sum_{i=1}^{N_{gen}} F_i\left(P_i^t\right) \tag{3}$$

where $F_i\ (P_i^t\ )$ denoted as diesel generator cost that should be minimized. a_i, b_i, and c_i are fuel coefficients. P_i^t is the capacity of each diesel generator. N_{gen} is number of diesel generators. P_{load}^t is the remainder load:

$$F_i\ (P_i^t\ ) = a_i + b_i \times\ P_i\ (t) + c \times\ P_i^2\ (t) \tag{4}$$

Subject to

$$\begin{cases} \sum_{i=1}^{N_{gen}} P_i^t = P_{load}^t \\ P_i^{min} \le\ P_i(t) \le P_i^{max} \end{cases} \tag{5}$$

VPP optimizes four diesel generators to shave the remainder of the load that could not be fully shaved by the EERs. Unit commitment approach based on dynamic programming is used to perform the optimization. Both fuel consumption coefficients and the capacity for each generator are provided in Table 1. Detailed information on optimization of unit commitment using dynamic programming can be found in [29].

Table 1. Capacities and coefficients for each diesel generator.

Gen No.	Capacity KW	a $	b $/MWh	c $/MWh^2
Gen 1	1250	1000	16.19	0.00048
Gen 2	600	970	17.26	0.00031
Gen 3	600	700	16.60	0.00200
Gen 4	750	680	16.50	0.00211

5. Formulation of the Proposed Method

The work here aims at optimizing the outputs of the local decentralized assets, which are covered in detail in Section 4, with the goal of reducing customers' consumption during peak periods by implementing peak load shaving. The electricity cost for LDCs is minimized by reducing the reliance on utility power during peak periods.

The objective function is used to minimize electricity costs. The problem is solved using mixed integer linear programming because it uses binary variables to control the charging/discharging of the utility battery [30]:

$$\text{Min}\, C_T \tag{6}$$

$$C_T = C_E + C_P \tag{7}$$

$$C_E = \zeta \cdot \sum_{i=1}^{N} P_{L\text{Shave}} \tag{8}$$

$$C_P = \alpha \cdot P_{\text{shave}} \tag{9}$$

Equations (6)–(9) represent the total charge C_T that includes energy charge C_E and peak charge C_P based on the peak load shaving. $PLShave$ and $Pshave$ are both indicators of the demand after performing peak shaving and maximum peak shaving during the billing cycle, respectively. Both ζ($/KWh)and α($/KW) represent the energy and peak charging rates, respectively. N denotes the 24 h load forecast:

$$\text{Soc}(t) = \text{Soc}(t-1) + \frac{\lambda \sum_{t-1}^{t} P_{batt}(t-1)dt - \mu \sum_{t-1}^{t} P_{batt}(t-1)dt}{\delta} \tag{10}$$

The state of charge $Soc(t)$ in Equation (10) is calculated based on the active power P_{batt} from the utility battery, as well as the charging λ and discharging μ efficiencies. In addition, the kWh rating of the energy battery rate is determined by using the δ parameter. The state of charge is initialized and updated every time:

$$\begin{cases} 0 \le CVR(t) \le CVR^{max} \\ \text{Soc}^{\text{min}} \le \text{Soc}(t) \le \text{Soc}^{\text{max}} \\ 0 \le P_G(t) \le P_G^{max} \\ Pbatt^{min} \le Pbatt(t) \le Pbatt^{max} \\ 0 \le P_{PV}(t) \le P_{PV}^{max} \\ 0 \le P_{DGi}(t) \le P_{DGi}^{max} \end{cases} \tag{11}$$

Equation (11) indicates that all local resources as seen in Section 4 are subject to certain operational constraints. The active power of the utility-scale battery, $Pbatt(t)$, is limited to 1.25 MW. In addition, the state of charge, $Soc(t)$, should range from 25% to 95%. The four diesel generators are as follows: P_{DGi} with varying capacity limits, as shown in Table 1. CVR also has a specific limit, as explained in Section 4.2. The PV capacity is also limited by the number of PV panels, as described in Section 4.3:

$$\sum_{i=1}^{n} P_i(t) + P_G(t) = P_L(t) \tag{12}$$

$$\sum_{i=1}^{n} P_i(t) = P_{PV}(t) \mp P_{batt}(t) + P_{Rbatt}(t) + P_{EWH}(t) + P_{HP}(t) + P_{BBH}(t) + P_{ETS}(t) + P_{DGi}(t) \quad (13)$$

Equation (12) represents the power balance between the main generation $P_G(t)$ (power plant), local assets $P_i(t)$ (explained in detail in Section 4), and load forecast $P_L(t)$ (forecast of customers' consumption over the next 24 h). A balance should be maintained between power generation and demand. There are two types of power generation: local resources (DERs and ESSs) and main generation (Power Plants). Our algorithm optimizes the capacity that is received from decentralized local resources, so that, when the local resources are maximized, the peak shaving level is maximized toward the threshold level. As a result of maximization of local resources, the main generation is reduced. Equation (13) shows the sum of the local assets. A minimum energy cost will be used for optimizing and coordinating these local assets, as represented in Equations (16)–(21). The priority asset will be selected based on the lowest energy cost at each point in time for each asset in the timeseries:

$$\begin{cases} \gamma_c(t)\, M \geq P_{batt} \\ 1 - \gamma_c(t)\, M \geq P_{batt} \\ \gamma_c(t) = 0 \; or \; 1 \end{cases} \quad (14)$$

$\gamma_c(t)$ represents the binary variable of the utility battery. If $\gamma_c(t) = 0$, the charging of the battery will be off, and the battery will be discharged. If $\gamma_c(t) = 1$, the discharging of the battery will be off and the battery will be charged. The purpose of $\gamma_c(t)$ is to simultaneously avoid charging and discharging the battery. M is the desired capacity of the battery to be charged or discharged. The available power for charging is provided by main generation (Power Plant). During the charging period, this power will be rated and paid by the utility:

$$\begin{cases} Pshave \leq Peak \\ Pshave \geq Pthreshold \\ P_G(t) \leq Pshave \end{cases} \quad (15)$$

Pshave is optimally set between the peak of the hourly load forecast and the desired level ($P_{threshold}$) because standalone aggregators often cannot fully shave the load. The main generation can therefore shave any additional load that is above the desired level. The main generation $P_G(t)$ is set to be less than or equal to *Pshave* because main generation will be reduced to a new peak shaving level when EERs are engaged.

Energy cost is calculated for each aggregators and resources based on the following equations:

$$Cost_T = Cost_{TInvest} + Cost_{EPC} \quad (16)$$

where $Cost_T$ and $Cost_{TInvest}$ denote the total cost of each aggregator and the investment of units, respectively. $Cost_{EPC}$ is the energy cost:

$$Cost_{TInvest} = Cost_U + Cost_{Mis} \quad (17)$$

where $Cost_U$ and $Cost_{Mis}$ denote unit cost and Miscellaneous cost for each aggregators, respectively,

$$Cost_U = Cost_{UEWH} + Cost_{UHP} + Cost_{UBBH} + Cost_{UETS} \quad (18)$$

where $Cost_{UEWH}$, $Cost_{UHP}$, $Cost_{UBBH}$, and $Cost_{UETS}$ denote unit cost of electric water heater, heat pump, baseboard heater, and electric thermal storage, respectively,

$$Cost_{Mis} = Cost_{MisIns} + Cost_{MisCont} + Cost_{MisMain} \quad (19)$$

where $Cost_{MisIns}$, $Cost_{MisCont}$, and $Cost_{MisMain}$ represent installation, controller, and maintenance costs for each aggregators, respectively:

$$Cost_{EPC} = (\beta \times P_c) \tag{20}$$

where β and P_c represent price rate on and off peak and power consumption during on and off peak for each aggregators, respectively,

$$Cost_{Thour} = \frac{N_U \times Cost_{TInvest}}{10 * 365 * 24} + (\beta \times P_c) \tag{21}$$

where $Cost_{Thour}$, N_U, and $Cost_{TInvest}$ are hourly total energy cost, number of units, and total cost of investment for each aggregators, respectively. The denominator of the above equation represents the aggregators performing maintenance every ten years calculated in hours. The above equation calculates the total cost of each aggregator. It consists of two components including the static and the dynamic components. The total investment cost is considered as a static component. The cost is determined based on both unit and miscellaneous costs. This part is almost constant and steady—in addition to that, the dynamic components which are computed based on the change in the power consumption during 24 h. Moreover, power consumption occurs when units of aggregators are charging. The charging rates in this section is published in [31]. Figure 2 describes the flowchart of the entire control algorithm process

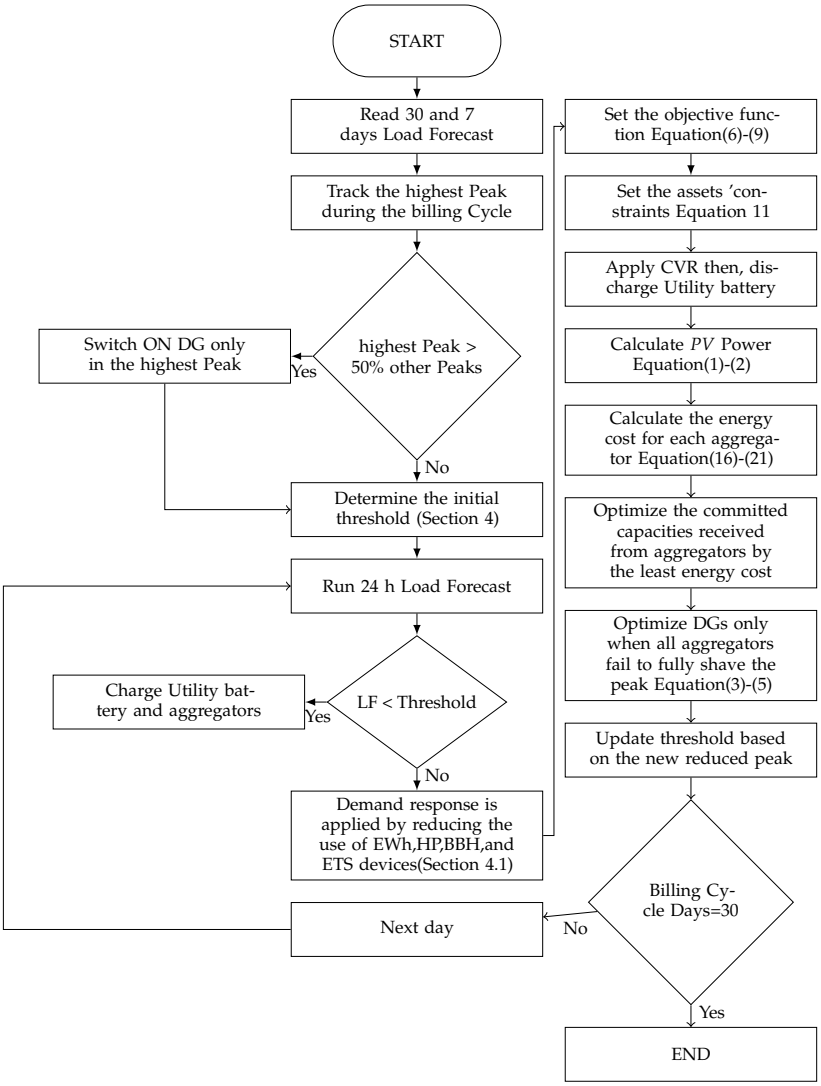


Figure 2. Flowchart of the proposed algorithm.

6. Case Study

A single-line diagram of the real Australian power distribution network used as the VPP is shown in Figure 3. There are additional resources being considered for this actual network. There are two solar farms at the VPP, a utility-scale battery with a capacity of 2.50 MWh and four residential batteries totaling 5 MW. There are four load substations totaling 80 MW, including 20.5 MW curtailable (the curtailment of the load is fully controlled by the VPP operator at \$400/MWh), and a 25 MW/90 MWh BESS. There are four diesel generators with four different capacities are shown in Table 1. Furthermore, decentralized energy storage systems are distributed around the distribution network and the information on numbers and capacities are demonstrated in Table 2.

Table 2. Capacities and coefficients for each diesel generator.

Cost \$	EWh	HP	BBH	ETS
Unit	400	1400	150	1500
Controller	200	150	200	200
Maintenance	150	400	150	400
Installation	1000	4000	400	2500
No. Units	1000	200	1200	500

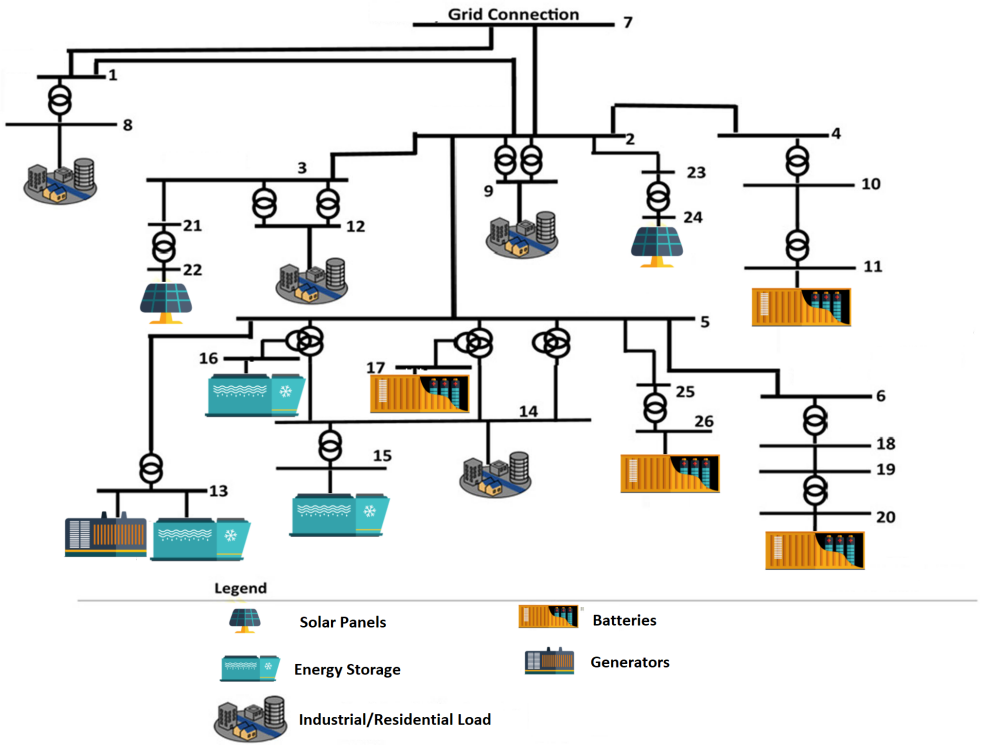


Figure 3. A real Australian power distribution network.

7. Results and Discussion

Four case studies are presented in this section explaining how peak load shaving works and how it can benefit LDCs economically. Each of these cases illustrates how EERs contribute differently each year, month, and day. A detailed discussion of the economic benefits and cost savings for LDCs is presented in this section as well.

7.1. Case 1: Hourly EERs Contributions for 1 February 2021

Table 1 illustrates the information about four diesel generators. A genetic algorithm is used to optimize diesel generators using a unit commitment approach. The operation of a diesel generator is classified as either OFF (zero capacity) or ON (full capacity). Table 1 pro-

vides the coefficient parameters as well. Table 2 summarizes the costs of four aggregators. Both HP and ETS are the most expensive in terms of unit and installation costs. Other costs are not significantly different. This table also shows the size of units used in the algorithm.

Figure 4 represents the output of different EERs and the state of charge of utility-scale and residential batteries. Moreover, it shows the dynamic response of solar irradiance and temperature on 1 February 2021. An optimized diesel generator is shown in Figure 4a. Due to fuel-related costs, four diesel generators are optimized as the last resource to fully shave the peak. Thus, four diesel generators switch ON/OFF based on the amount needed to completely shave the peak. The diesel generators 1, 3, and 4 are on, and generator 2 is off for the specific peak shown in Figure 5. Figure 4b shows the contribution of a utility-scale battery. The battery's capacity is 2.50 MWh, and its maximum output power is always at 1.25 MW, so, in two hours, it will be fully depleted. Figure 4c illustrates the contributions of the four aggregators. The yellow area shows the capacity reserved by aggregators for peak load shaving as requested by VPPs. Other parts show how these aggregators operate, such as pre-charging before peak and post-charging after peak periods. Figure 4d represents how the algorithm works. The algorithm reads the peak of the 24-h load forecast and looks for contributions from EERs to reduce the peak level. More EERs contributions lead to more peak shaving. The contribution of residential batteries is shown in Figure 4e. The number of residential batteries in this paper is 50. Residential batteries contributed 0.537 MWh, as is apparent from Table 3. Figure 4f represents the dynamic behavior of solar power during the day. Due to low radiation in the area, solar contributes a very small percentage compared to other EERs. Figure 4g shows the state of charge of 50 residential batteries distributed across the real Australian distribution network. It took four hours for the residential batteries to fully charge (6:00 a.m. to 10:00 a.m.) and discharge (11:00 a.m. to 3:00 p.m.) during the peak time. Figure 4h illustrates solar irradiance. Most of the irradiance occurred between 8:00 a.m. and 8:00 p.m. on 1 February 2021. Based on Figure 4i, there is a low irradiance during the day due to lower temperatures. A utility-scale battery's state of charge is shown in Figure 4j. The utility-scale battery is modeled to fully charge and discharge within 2 h due to its capacity of 2.50 MWh and maximum output power of 1.25 MW.

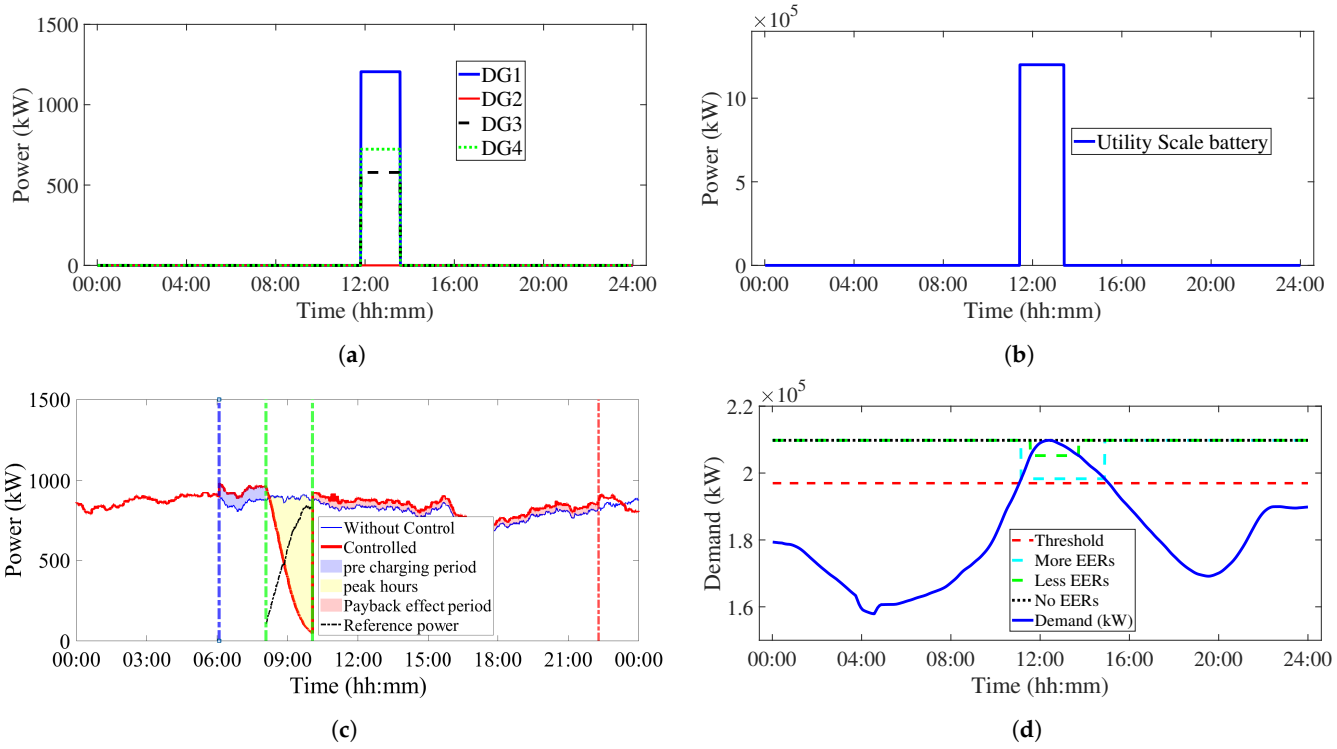


Figure 4. *Cont.*

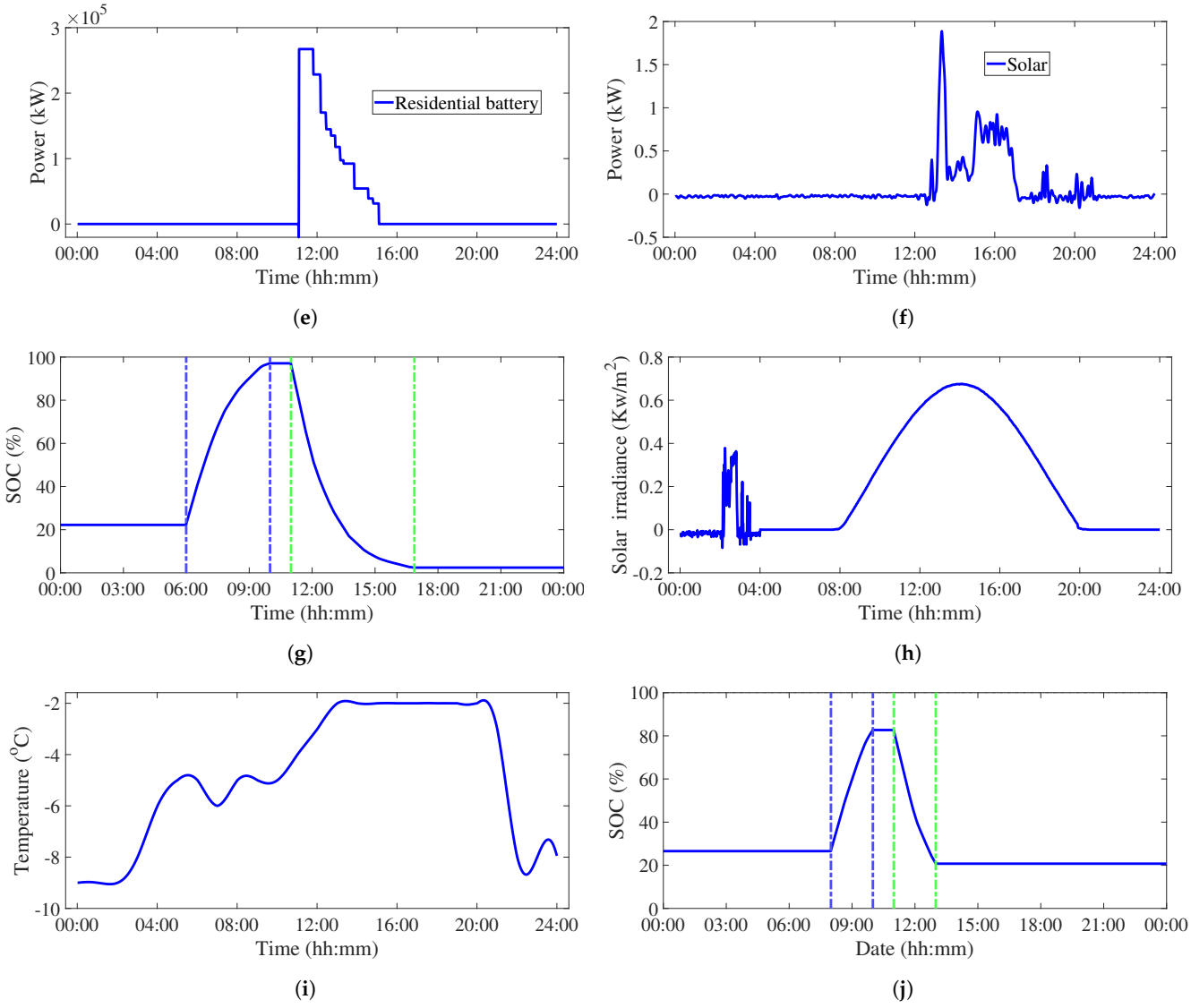


Figure 4. (**a**) Diesel generators; (**b**) utility scale battery; (**c**) aggregators; (**d**) peak shaving algorithm; (**e**) residential battery; (**f**) solar power; (**g**) RB state of charge; (**h**) solar irradiance; (**i**) area temperature on 1 February 2021; (**j**) UB state of charge.

Table 3. Contributions of EERs for Monthly Peak Load Shaving.

February 2021	Peak Type	CVR MWh	UBatt MWh	RBatt MWh	BBH MWh	HP MWh	Diesel MWh	EWh MWh	ETS MWh
1	Morning	8.816	2.380	0.537	0.871	2.116	4.219	0.941	0.206
2	Morning	2.350	1.340	0	0	0	0	0	0
14	Morning	1.766	0	0	0	0	0	0	0
14	Evening	2.345	0	0	0	0	0	0	0
15	Morning	7.356	2.380	0.551	0.915	2.118	0	0.976	0.181
16	Morning	2.505	1.660	0	0	0	0	0	0
25	Morning	2.400	0	0	0	0	0	0	0
25	Evening	2.453	0	0	0	0	0	0	0
March 1	Morning	1.414	0	0	0	0	0	0	0

7.2. Case 2: Daily Peak Load Shaving for the Month of February 2021

The billing cycle of February is chosen due to the highest consumption in 2021. The table below shows the peak load shaving for February 2021. There were two peak shavings

on 14 and 25 February: one in the morning and one in the evening. Other EERs including utility-scale batteries were off because CVR was able to fully shave the peak. The EERs will be optimized based on the least-cost option, so CVR and utility-scale battery are both given priority due to its lower cost. A second priority will be given to aggregators, and diesel generators will be used only when all other EERs fail to completely shave the peak. Figure 5 shows the 24-h demand. The yellow area represents EERs, and the blue area represents the main generation. There was a peak between 11:00 a.m. and 3:00 p.m. on 1 February. The duration of the peak is four hours. The red line represents the threshold, so any load above the threshold should be shaved. As it can be seen, EERs have completely shaved the peak. In addition, there were also three peaks on 2 March. The first peak occurred between 2:00 p.m. and 8:00 p.m., and it lasted for six hours. It can be seen that the EERs cannot fully shave the demand as the blue area is still visible. Furthermore, the EERs completely shaved the second peak from 8:30 p.m. to 10:00 p.m. on the same day. Another consecutive peak occurred near midnight. The duration of the third peak is less than an hour. Figure 5d is zoomed in to clearly show the small third peak. The goal is to shave off any peaks that last longer than 15 min using this method. The algorithm is capable of tracking and shaving more than one peak per day.

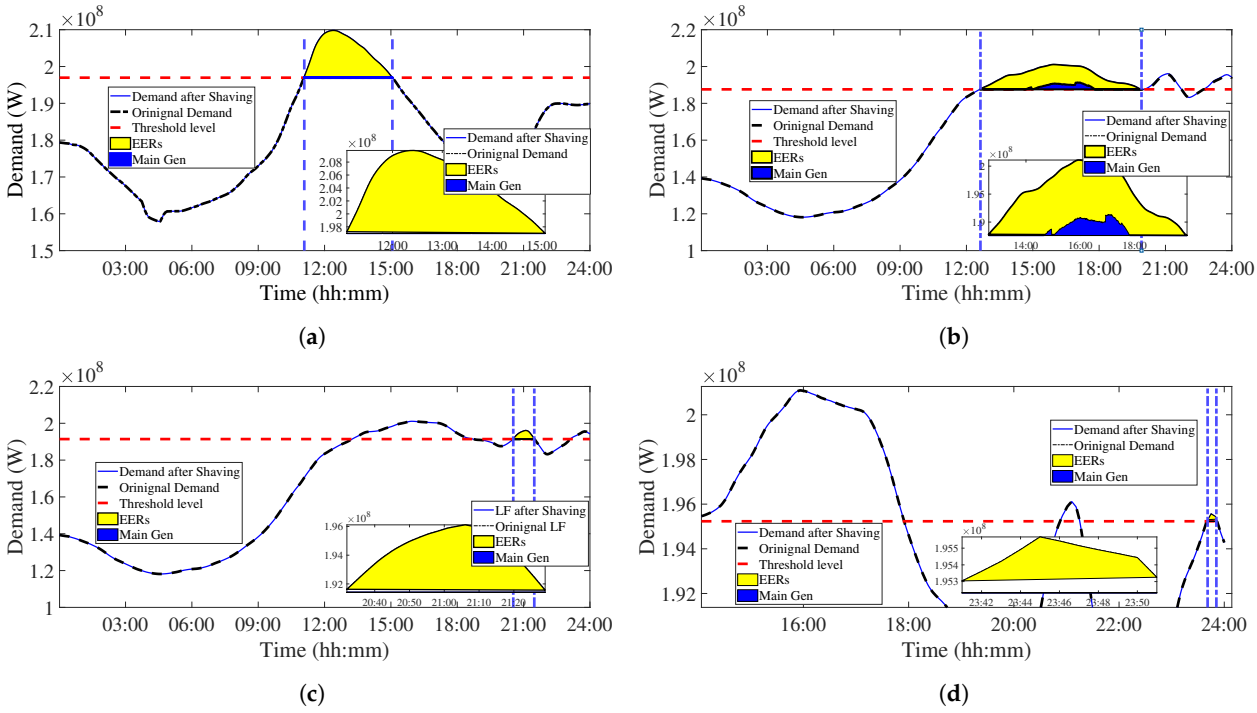


Figure 5. (**a**) First peak shave on 1 February; (**b**) first peak shave on 2 March; (**c**) second peak shave on 2 March; (**d**) third peak shave on 2 March.

The contribution of each EERs on 1 February 2021 is shown in Figure 6a. The CVR contributed 44%, which is the largest, followed by 21% for diesel generators. Utility-scale batteries contributed by 12%, and other cheap EERs contributed from 1% to 10%. Furthermore, Figure 6b represents 100% peak shaving by EERs. Figure 7 represents the entire billing cycle for February 2021. Consumption is higher at the beginning and middle of the billing cycle, so most peak shavings occurred at those times. The highest peak was on 15 February. A detailed description of peak shavings can be found in Table 3.

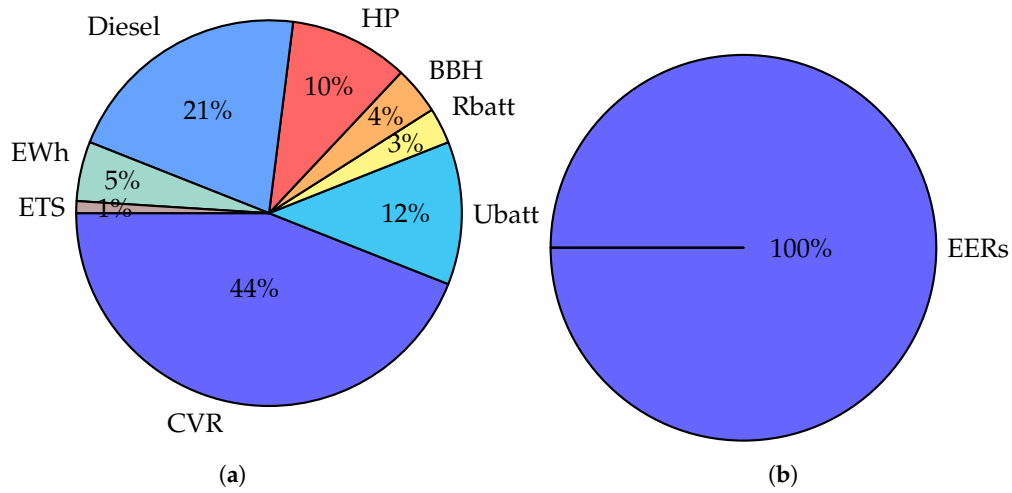


Figure 6. (**a**) Contributions of EERs; (**b**) total contributions of EERs and main generation.

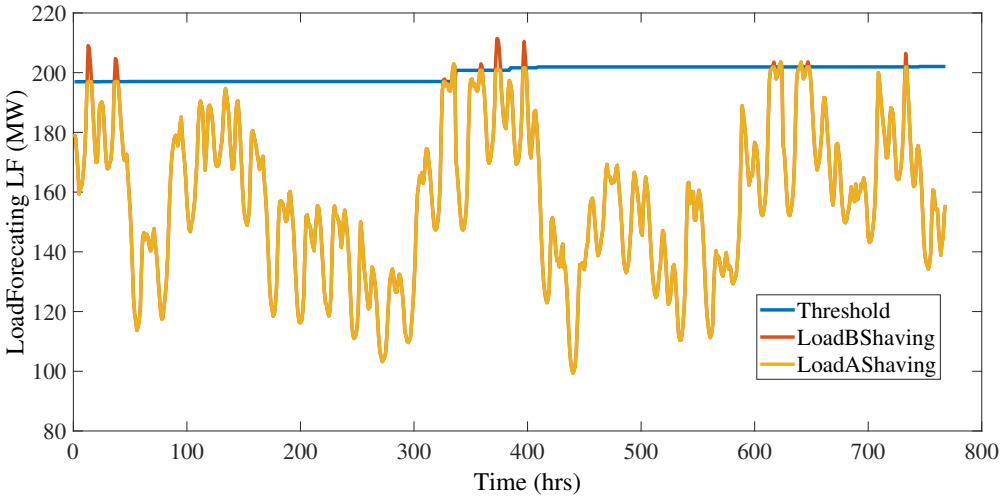


Figure 7. Billing cycle for February 2021.

7.3. Case 3: Monthly Peak Load Shaving for the Year of 2021

Table 4 shows the contributions of each EERs for the monthly peak load shaving. The optimization technique optimizes the EERs based on the lowest cost. CVR, utility, and residential batteries are the first selection to shave the load since there is lower cost. Other priorities are given to aggregators, which are optimized based on the energy cost. Diesel generators will be the last choice due to its fuel-related costs. The table includes the number of peaks for each billing cycle. It is clear that June has the highest number of peaks. Despite that, June's cost saving is not high due to low consumption. As a result, the number of peaks does not directly correlate with cost savings. CVR, 21.92 MWh and utility-scale battery, 2.74 MWh were used in September since they are our first choices. Other resources turned off to be reserved for other peak shavings. In addition, December has the highest use of both CVR, 81.48 MWh, and utility-scale battery, 8.96 MWh, but that did not fully shave the peak load, which requires other resources such as aggregators to engage to fully shave the peak. A high CVR capacity indicates high consumption, so winter CVR capacity tends to be higher than summer.

Table 4. Contributions of EERs for monthly peak load shaving.

No. Peaks	Month 2021	CVR MWh	UBatt MWh	RBatt MWh	BBH MWh	HP MWh	Diesel MWh	EWh MWh	ETS MWh
11	January	58.8059	8.6400	2.1235	3.5592	9.2995	1.5780	3.8472	0.9684
9	February	31.4093	7.7600	1.0878	1.7859	4.2348	4.2198	1.9166	0.3865
6	March	31.2262	4.2800	1.1038	1.7414	5.5876	3.0176	2.0155	1.8916
5	April	36.0006	6.4400	1.6511	2.8061	8.9259	7.2819	2.9904	2.1631
8	May	41.1970	8.3400	2.0687	4.0062	11.2082	2.3523	3.1062	1.0817
18	June	43.4794	2.3800	1.2925	0.5972	1.9393	1.8786	0.9876	0.5483
11	July	42.0988	7.1400	1.7247	1.9152	3.4082	1.9592	2.1908	1.9275
11	August	32.9884	7.6600	1.1498	1.9299	7.4148	0	2.1427	2.0351
9	September	21.9147	2.7400	0	0	0	0	0	0
8	October	17.8657	4.7600	1.0829	1.8773	5.1234	3.1746	1.9168	0.5371
10	November	23.8643	1.8200	0.1259	1.9293	1.8548	0	0.9667	0.7447
10	December	81.4757	8.9600	1.8325	5.1198	11.8830	2.0409	3.9998	2.6960

Figure 8 represents Table 4. The approach only used 89% of CVR and 11% of utility-scale battery in September due to its capability to provide full load shaving. Both August and November did not use diesel generators due to their fuel-related costs, so other cheap resources completely shaved the peak load. The second reason is that diesel generators are subjected to time constraints, so, if the highest peak is not significantly higher than other peaks, diesel generators will not be reserved for the highest peak, leading to lower billing cycle cost savings. Heat pumps have the highest percentage of contribution among other aggregators.

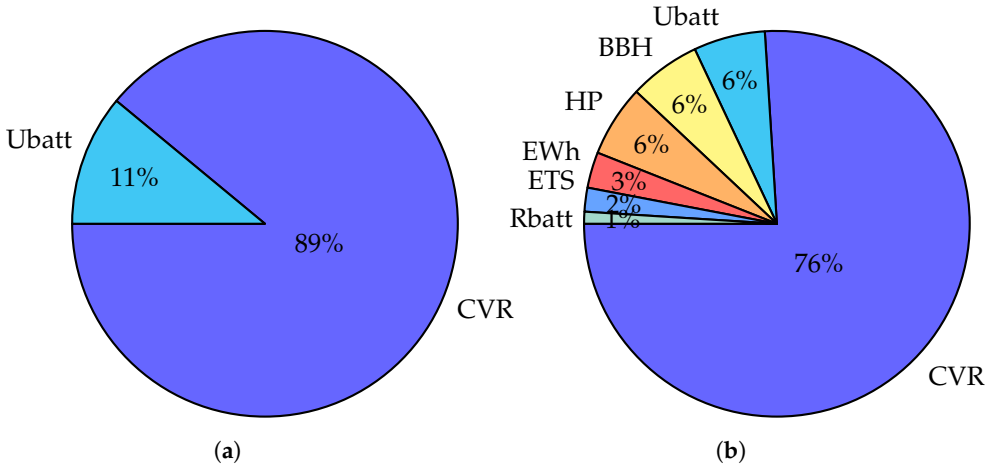


Figure 8. (**a**) Contributions of EERs for peak load shaving in September 2021; (**b**) contributions of EERs for peak load shaving in November 2021.

7.4. Case4: Monthly Economical Analysis of Peak Load Shaving in 2021

Table 5 shows the highest peaks for each billing cycle in 2021. As can be seen, the highest peak in 2021 was in February, 212.27 MW. The second highest peak in 2021 is in March, 201.4 MW, followed by the third highest peak in December, 195.86 MW. By contrast, summer months have the lowest peak except for August, which is somewhat greater than other summer months. Both June and July have the lowest peak compared to the rest of the year.

Table 5. Maximum peaks and for each billing cycle of peak load shaving.

Peak Dates	January 21	February 15	March 2	April 4	May 8	June 1	July 15	August 25	September 9	October 25	November 29	December 24
Peak MW	185	212	201	148	117	91	93	100	94	109	164	195
Threshold MW	175	200	190	138	112	87	87	97	91	103	159	180

Figure 9 illustrates how cost savings are calculated based on two factors. The peak load and off-peak load have two different electricity prices. First, multiply the maximum peak by the kW rate and, second, multiply the total consumption during the billing cycle by the kWh rate. These rates are provided by the Australian Energy Market Operator (AEMO). The two factors should be added together to compute the total cost. Cost savings determined by comparing the total cost before and after peak shaving and will be calculated as the difference between them. As can be seen from the figure, February has the highest cost savings of AUD 123,000, followed by December with AUD 115,200. June has the lowest cost savings of AUD 10,600 compared to the rest of 2021. Additionally, there is a slight difference in cost savings during the summer months since consumption varies less. In the winter, however, cost savings vary significantly due to fluctuations in consumption. To sum up, the total cost savings were AUD 632,822 in 2021.

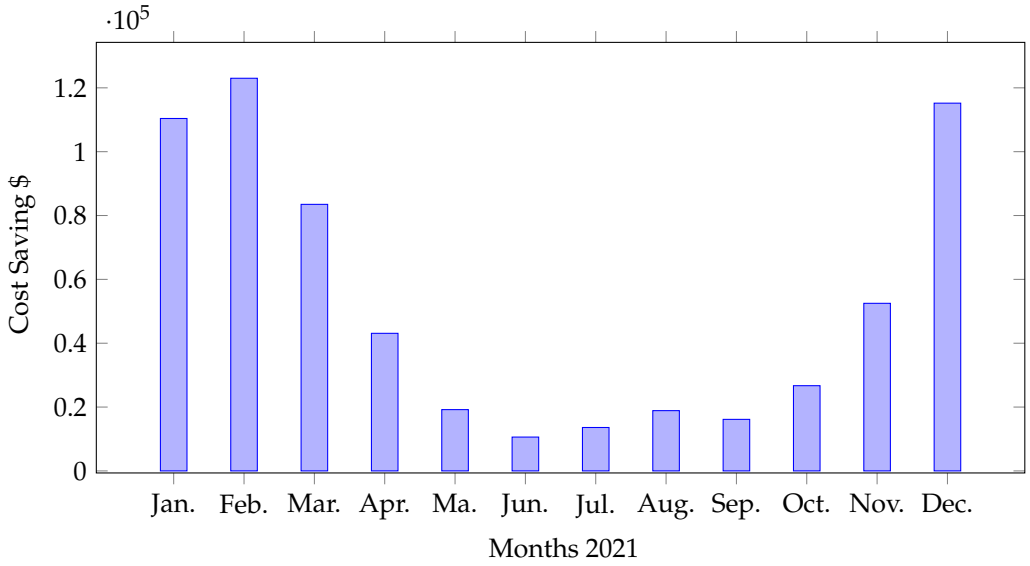


Figure 9. Monthly cost saving for 2021 peak load shaving.

8. Conclusions

The work presents an effective algorithm to control embedded energy resources in order to optimize electricity cost for local distribution networks. This algorithm has proven to be capable of reducing peak demand in real-time scenarios. Up to three daily peaks can be shaved using this mechanism. Assets are prioritized by the control algorithm. CVR is the first option selected because it has no charging cost, batteries are the second option, aggregators are the third option, and then diesel generators are the last option because of fuel-related costs. Different aggregators are optimized based on lower energy cost. This paper examines four different case scenarios. The first case shows the different contributions of EERs during the peak periods. Peak load shaving is performed for the entire year of 2021 as shown in the second case. The third case illustrates peak shaving performance in specific months with details on each EER contribution. The economic analysis of peak shaving for the entire year 2021 is determined to assess the overall benefit of the algorithm. The presented algorithm proved the capability of shaving up to three daily peaks and providing significant cost savings of more than AUD 600,000 in 2021. This paper will be extended in the future to include the degradation of PV power over the years and the impact of greenhouse gas emissions (CO_2) produced by diesel generators.

Author Contributions: Conceptualization, H.M.; Formal analysis, H.M.; Methodology, H.M.; Software, H.M.; Supervision, E.C.G. and J.L.C.B.; Writing—original draft, H.M.; Writing—review & editing, H.M. All authors have read and agreed to the published version of the manuscript.

Funding: This research was funded by Emera & NB Power Research Center for Smart Grid Technologies at University of New Brunswick https://www.unb.ca/smartgrid (accessed on 12 October 2022).

Data Availability Statement: "Australian Energy Market Operator AEMO" at https://aemo.com.au/en (accessed on 8 August 2022).

Conflicts of Interest: The authors declare no conflict of interest.

Abbreviations

The following abbreviations are used in this manuscript:

VPP	Virtual Power Plant
BESSs	Battery Energy Storage Systems
DERs	Distributed Energy Resources
EERs	Embedded Energy Resources
ESSs	Energy Systems Storage
BBH	Baseboard Heater
EWh	Electric Water Heater
HP	Heat Pump
RB	Residential Battery
LF	Load Forecast
ETS	Electric Thermal Energy Storage
Ubatt	Utility Scale battery
Rbatt	Residential battery
CVR	Conservation Voltage Reduction
LoadBShaving	Load before shaving
LoadAShaving	Load after shaving
DG	Diesel Generator
AGGs	Aggregators
AEMO	Australian Energy Market Operator
EV2G	Electric Vehicle to Grid

References

1. Uddin, M.; Romlie, M.F.; Abdullah, M.F.; Abd Halim, S.; Kwang, T.C. A review on peak load shaving strategies. *Renew. Sustain. Energy Rev.* **2018**, *82*, 3323–3332. [CrossRef]
2. Lu, C.; Xu, H.; Pan, X.; Song, J. Optimal sizing and control of battery energy storage system for peak load shaving. *Energies* **2014**, *7*, 8396–8410. [CrossRef]
3. Singh, S.; Singh, S.P. Peak load relief in MV/LV distribution networks through smart grid-enabled CVR with droop control EV2G reactive power support. In Proceedings of the 2018 International Conference on Power, Instrumentation, Control and Computing (PICC), Thrissur, India, 18–20 January 2018.
4. Arora, S.; Satsangi, S.; Kaur, S.; Khanna, R. Substation demand reduction by CVR enabled intelligent PV inverter control functions in distribution systems. *Int. Trans. Electr. Energy Syst.* **2021**, *31*, 12724. [CrossRef]
5. Chowdhury, B.H. Central-station photovoltaic plant with energy storage for utility peak load leveling. In Proceedings of the 24th Intersociety Energy Conversion Engineering Conference, Washington, DC, USA, 6–11 August 1989.
6. Mahmud, K.; Hossain, M.J.; Town, G.E. Peak-load reduction by coordinated response of photovoltaics, battery storage, and electric vehicles. *IEEE Access* **2018**, *6*, 29353–29365. [CrossRef]
7. Wang, Z.; Wang, S. Grid power peak shaving and valley filling using vehicle-to-grid systems. *IEEE Trans. Power Deliv.* **2013**, *28*, 1822–1829. [CrossRef]
8. Ghosh, D.P.; Thomas, R.J.; Wicker, S.B. A privacy-aware design for the vehicle-to-grid framework. In Proceedings of the 2013 46th Hawaii International Conference on System Sciences,Wailea, HI, USA, 7–10 January 2013.
9. López, M.A.; De La Torre, S.; Martín, S.; Aguado, J.A. Demand-side management in smart grid operation considering electric vehicles load shifting and vehicle-to-grid support. *Int. J. Electr. Power Energy Syst.* **2015**, *64*, 689–698. [CrossRef]
10. Baniasadi, A.; Habibi, D.; Al-Saedi, W.; Masoum, M.A.; Das, C.K.; Mousavi, N. Optimal sizing design and operation of electrical and thermal energy storage systems in smart buildings. *J. Energy Storage* **2020**, *28*, 101186. [CrossRef]
11. Lavrova, O.; Cheng, F.; Abdollahy, S.; Barsun, H.; Mammoli, A.; Dreisigmayer, D.; Willard, S.; Arellano, B.; Van Zeyl, C. Analysis of battery storage utilization for load shifting and peak smoothing on a distribution feeder in New Mexico. In Proceedings of the 2012 IEEE PES Innovative Smart Grid Technologies (ISGT), Washington, DC, USA, 16–20 January 2012; pp. 1–6.
12. Vanhoudt, D.; Geysen, D.; Claessens, B.; Leemans, F.; Jespers, L.; Van Bael, J. An actively controlled residential heat pump: Potential on peak shaving and maximization of self-consumption of renewable energy. *Renew. Energy* **2014**, *63*, 531–543. [CrossRef]

13. Sepulveda, A.; Paull, L.; Morsi, W.G.; Li, H.; Diduch, C.P.; Chang, L. A novel demand side management program using water heaters and particle swarm optimization. In Proceeding of the 2010 IEEE Electrical Power & Energy Conference, Halifax, NS, Canada, 25–27 August 2010.
14. Belov, A.; Vasenev, A.; Kartak, V.; Meratnia, N.; Havinga, P.J. Peak load reduction of multiple water heaters: Respecting consumer comfort and money savings. In Proceeding of the 2016 IEEE Online Conference on Green Communications (OnlineGreenComm), Piscataway, NJ, USA, 14 November–17 December 2016.
15. Martins, R.; Hesse, H.C.; Jungbauer, J.; Vorbuchner, T.; Musilek, P. Optimal Component Sizing for Peak Shaving in Battery Energy Storage System for Industrial Applications. *Energies* **2018**, *11*, 2048. [CrossRef]
16. Cheng, X.; Feng, S.; Huang, Y.; Wang, J. A New Peak-Shaving Model Based on Mixed Integer Linear Programming with Variable Peak-Shaving Order. *Energies* **2021**, *14*, 887. [CrossRef]
17. Liao, S.; Zhang, Y.; Liu, B.; Liu, Z.; Fang, Z.; Li, S. Short-Term Peak-Shaving Operation of Head-Sensitive Cascaded Hydropower Plants Based on Spillage Adjustment. *Water* **2020**, *12*, 3438. [CrossRef]
18. Tchagang, A.; Yoo, Y. V2B/V2G on Energy Cost and Battery Degradation under Different Driving Scenarios, Peak Shaving, and Frequency Regulations. *World Electr. Veh. J.* **2020**, *11*, 14. [CrossRef]
19. Gliński, M.; Bojesen, C.; Rybiński, W.; Bykuć, S. Modelling of the Biomass mCHP Unit for Power Peak Shaving in the Local Electrical Grid. *Energies* **2019**, *12*, 458. [CrossRef]
20. Odkhuu, N.; Lee, K.-B.A.; Ahmed, M.; Kim, Y.-C. Optimal Energy Management of V2B with RES and ESS for Peak Load Minimization. *Appl. Sci.* **2018**, *8*, 2125. [CrossRef]
21. Gelleschus, R.; Böttiger, M.; Bocklisch, T. Optimization-Based Control Concept with Feed-in and Demand Peak Shaving for a PV Battery Heat Pump Heat Storage System. *Energies* **2019**, *12*, 2098. [CrossRef]
22. Bignucolo, F.; Caldon, R.; Prandoni, V.; Spelta, S.; Vezzola, M. The voltage control on MV distribution networks with aggregated DG units (VPP). In Proceeding of the 41st International Universities Power Engineering Conference, Newcastle upon Tyne, UK, 6–8 September 2006.
23. Pudjianto, D.; Ramsay, C.; Strbac, G. Virtual Power Plant and System Integration of Distributed Energy Resources. *IET Renew. Power Gener.* **2007**, *1*, 10–16. [CrossRef]
24. Dauensteiner, A. *European Virtual Fuel Cell Power Plant*; Management Summary Report; Germany, NNE5-2000-208, 2007.
25. Pudjianto, D.; Ramsay, C.; Strbac, G.; Durstewitz, M. The virtual power plant: Enabling integration of distributed generation and demand. *Fenix Bull.* **2008**, *2*, 10–16.
26. Braun, M. Virtual power plants in real applications-pilot demonstrations in Spain and England as part of the European project FENIX. In Proceedings of the Internationaler ETG Kongress, Düsseldorf, Germany, 27–28 October 2009.
27. Shafieisarvestani, A. Homogeneous Load Aggregation: Implementation and Control For Smart Grid Functions. Master's Thesis, UNB, Fredericton, NB, Canada, 2022.
28. Kharrich, M.; Kamel, S.; Hassan, M.H.; ElSayed, S.K.; Taha, I.B. An improved heap-based optimizer for optimal design of a hybrid microgrid considering reliability and availability constraints. *Sustainability* **2021**, *13*, 10419. [CrossRef]
29. Chaudhari, S.; Killekar, S.; Mahadik, A.; Meerakrishna, N.; Divya, M. A review of unit commitment problem using dynamic programming. In Proceedings of the IEEE International Conference on Nascent Technologies in Engineering (ICNTE), Navi Mumbai, India, 4–5 January 2019.
30. Danish, S.M.S.; Ahmadi, M.; Danish, M.S.S.; Mandal, P.; Yona, A.; Senjyu, T. A coherent strategy for peak load shaving using energy storage systems. *J. Energy Storage* **2020**, *32*, 101823. [CrossRef]
31. AEMO, Melbourne, Australia. National Electricity Market: Average Daily Prices. Available online: www.aemo.com.au/Electricity/National-Electricity-Market-NEM/Data-dashboard (accessed on 8 August 2022).